Cost-benefit analysis of integrated energy system planning considering demand response

Yue Xiang[a], Hanhu Cai[a], Chenghong Gu[b], Xiaodong Shen[a*]

[a] College of Electrical Engineering, Sichuan University, Chengdu 610065, China
[b] Department of Electronic and Electrical Engineering, University of Bath, Bath BA2 7AY, UK

Abstract The power-gas-coupling can realize the cascade utilization of energy in the integrated energy system, which is conducive to improving the utilization of energy and reducing pollution gases emissions. With the installation of smart metering, two-way communication between suppliers and consumers is feasible, which enables the implementation of demand response. A generic optimal planning model is proposed to assess the economic and environmental benefits of the capacity allocation of the grid-connected integrated energy system considering both price-based demand response and incentive-based demand response respectively. The optimal planning problem is formulated as a mixed-integer linear programming model with the objective to minimize the total annual cost. The results from three configuration modes are compared in the case study, which illustrate the economic and environmental benefits from demand response. In addition, the impact of the sales capacity constraint on the grid and the fluctuation of electricity and gas prices on the planning of the integrated energy system are also extensively studied considering demand response.

Keywords: capacity planning; integrated energy system; demand response; cost-benefit analysis; sensitivity analysis

Nomenclature

Indices

STC	Standard test conditions(Cell temperature 25℃, irradiance 1kW/m2)
PV	Photovoltaic
WT	Wind turbine
CHP	Combined heating and power supply
O&M	Operation and maintenance
Y_{PV}	Rated capacity of PV(kW)
G_T	Solar radiation (kW/m2)
T_{C}	Ambient temperature(℃)
P_W	Generation power of WT(kW)

Variables

$V_{\mathrm{G},i}^{\mathrm{cap}}$	Capacity for equipment *i* (kW, kWh)
δ_i	Binary variable to determine the operation status of equipment *i*
δ_{chg} / δ_{dsg}	Binary variable representing charge/ discharge of storage battery
δ_{buy} / δ_{sale}	Binary variable representing electricity purchase/sale
$P_{t,\mathrm{in}}^{\mathrm{con,AC}}$	Input power of the AC sides of convertor(kW)
$P_{t,\mathrm{out}}^{\mathrm{con,DC}}$	Output power of the DC sides of convertor(kW)
P_t^{MT}	Electrical output for MT(kW)
P_t^{chg} / P_t^{dsg}	Charging and discharging power of battery(kW)
P_t^{buy} / P_t^{sale}	Power that purchased from grid and sold into the grid(kW)

*Corresponding author: shengxd@scu.edu.cn

$\overline{P}_W$	Rated power of WT(kW)	H_t^{GB}	Heat output of gas boiler(kW)
v_{ci}	Cut-in wind speed(m/s)	ξ_i	Auxiliary variable in linearization (kW)
v_{co}	Cut-out wind speed(m/s)	**Constants**	
$\overline{v}$	Rated wind speed(m/s)	G_{STC}	Solar radiation incident at STC (kW/m2)
F_t^{CHP}	Gas consumption rate of CHP (m³/hr)	f_{PV}	Derating factor of PV(%)
Q_t^{CHP}	Heat produced by CHP(MJ)	T_{STC}	Incident radiation at STC(kW/m^2)
H_t^{CHP}	Heat output of CHP(kW)	α_{P}	Temperature coefficient (%/°C)
Y_{MT}	Nominal capacity of MT(kW)	η^{cov}	Efficiency of converter
E^{t+1}/E^t	Energy stored at time slots t+1 and t(kWh)	c_0	Fuel intercept coefficient (m³/kW/hr)
F_t^{boiler}	Gas consumption rate of boiler(m³/hr)	c_1	Fuel curve slope (m³/kWh/hr)
L_t^{d0}	Load value(kW)	ς_{hr}	Heat recovery ratio
L_t^{pbdr}	Load after implementing PBDR(kW)	ρ_{gas}	Density of natural gas(kg/m^3)
η_{kt}	Load response rate under k tap at time slot t	LHV_{gas}	The lower heating value of gas(MJ/kg)
ΔL_t^{pbdr}	Load participated in PBDR(kW)	δ_{bat}	Standby energy loss ratio of storage battery
$\Delta L_t^{pbdr,\max}$	Maximum allowable values for ΔL_t^{pbdr}	η^c/η^d	Charging and discharging efficiency of storage battery
α_{kt}	Identification indices of the price of electricity	η_{boiler}	Conversion efficiency of the boiler
F_{tot}	Total annual planning cost(yuan)	j/R_{proj}	Discount rate/ project cycle
F_1	Economic cost(yuan)	$CRF(j,R_{\mathrm{proj}})$	Capital recovery factor
F_2	Environmental cost(yuan)	a_i/b_i	Unit investment/replacement cost (yuan/ kW, yuan/kWh)
$CRF(j,R_{\mathrm{proj}})$	Capital recovery factor	π^i	Unit price of the pollutant i(yuan/t)
M	Number of categories of elements	y_i	Replacement year of device i(yr)
S_i	Residual value left by component i(yuan)	$d_{\mathrm{CHP}}^{\mathrm{gas},i}$	Emissions of the pollutant i from CHP(g/m^3)
$C_{\mathrm{op}}^{\mathrm{fixed}}$	O&M cost related to devices(yuan)	$d_{\mathrm{boiler}}^{\mathrm{gas},i}$	Emissions of the pollutant i from boiler(g/m^3)
C_{IBDR}	Compensation cost related to IBDR(yuan)	d_{grid}^i	Emission of the pollutant i from the grid(g/kWh)
t_{yr}	Annual operating time of MT(h)	$v_i^{\min}$	Minimum output power coefficient of equipment i
λ^{IBDR}	Compensation price of IBDR (yuan/ kWh)	$P_{\max}^{\mathrm{bat}}$	Maximum charging/discharging power(kW)
$P_t^{\mathrm{E}\text{-}i}$	Output of equipment i(kW)	$G^{\max}$	Maximum sales power (kW)
c_t^{buy} / c_t^{sale}	Buy and sale prices of electricity (yuan/ kWh)	$E^{\max}/E^{\min}$	Maximal/inimal capacity of energy storage battery(kWh)
$P_m^{\max}$	Maximum power demand in mouth m (kW)	$V_{G,i}^{cap,\max}/V_{G,i}^{cap,\min}$	Maximal/minimal capacity of equipment i(kW,kWh)
c^{demand}	Power demand charge(yuan/kW)		

1 Introduction

Integrated energy system(IES), the direction of energy development and the foundation of the future energy internet [1], uses advanced energy conversion and transmission technologies to convert solar energy, wind energy, geothermal energy,

natural gas and other resources into cold, heat, electricity and other forms of energy to improve the comprehensive utilization efficiency of energy and enhance the flexibility, safety, economy and self-healing capability of the energy supply [2]. Planning and design is one core aspect of the IES, which is directly related to the environmental protection, economy, and reliability of the system [3]. An effective IES planning can improve energy supply reliability, and meet the requirements for energy quality, facilitate governmental ambition in environmental protection.

Existing research on IES planning mainly focuses on capacity planning of distributed energy resources(DER), micro-grids and power-gas-coupling systems. Some researches consider planning from the perspective of economic cost. For example, Chao Qin et al. brought in the robust optimization theory, a multi-objective robust optimization model for IES is constructed based on minimizing energy cost and the wind curtailment[4]. Yang Y et al. proposed an mixed integer linear programming model to design a district-scale DER[5]. Quashie M et al. proposed a bi-level formulation for a coupled microgrid power and reserve capacity planning problem [6], and Jaesung J et al. proposed a technique for the optimal planning and design of hybrid renewable energy system for microgrid applications[7]. In addition, some researches consider the impact of environmental costs on system planning. For example, Patrizia S et al. proposed a framework for planning and design of smart multi energy systems considering environmental performance maximization[8]. Tengfei Ma et al. proposed a optimal planning model to design multi energy system, which can obtain the optimal structure configuration and energy management strategies [9]. However, the above studies did not fully consider the integration of operations and planning, and demand side response to further improve the economy and environmental protection.

Demand response (DR) is described as consumer's interest to shift or reduce their electricity usage from peak time to off-peak time in response to time-based price rates or incentive-based programs[10]. With smart metering gradually penetrating at user end [11], the two-way real-time communication technologies will significantly: i) improve the interactive response between network operators and end users[12], and ii) realize timely transfer of electricity price information and related incentives to users, enabling DR to have more efficient load control capability and accurately perceiving any changes and response behaviors of end users [13]. This provides conditions for the implementation of demand response.

Many studies on IES only consider the optimal operation. For example, the effect of flexible electrical load on IES economic benefit is studied, and IES' economic scheduling based on DR is established [14]. In [15], a DR uncertainty model based on Z-number method is established by analyzing the adjustable characteristics of different types of energy load under the regional electro-pneumatic coupling system. An electric/thermal integrated demand response(IDR) based on

pluripotency is proposed from the perspective of industrial users [16]. Yongli Wang, et al presents an optimal operation model of the IES considering the response of energy price [17]. However, implementing a DR strategy based on a planned system may introduce new problems, such as the massive curtailment of wind and solar, etc. The device capacity composition of a given system may not be the optimal structure to implement a DR strategy. Therefore, it is necessary to consider the DR while planning.

In order to reduce the curtailment of wind and solar power, this paper considers DR in the process of planning, and illustrates the economic and environmental benefits of DR by comparing the planning results. In this paper, there are two types of DR that are considered in planning. The first type is price-based demand response (PBDR) [18], which is used to show the impact of consumers' participation in load curve modification. There are many factors that users participate in the response to electricity demand. Kangping Li, et al explore the impact of household characteristics on PDR under TOU price by building an association rule mining based quantitative analysis framework[19]. But in this paper, price elasticity of demand [20] is defined as sensitivity of demand quantity with respect to change in price; The second aspect is incentive-based demand response (IBDR) [21], that is, a fixed or time-varying incentive payment is offered to the consumers to increase or diminish their load.

Some researches consider electric/thermal integrated demand response in the planning. For example, an 0-1 mixed integer linear programming model is established considering integrated demand response and the operating constraints of energy hub[22]. In [23], the energy supply side thermal/electrical load curve are smoothed by considering the electric/thermal load demand response and the supply and demand bilateral thermal/electrical coupling in the microgrid energy planning, but the microgrid only runs under off-grid conditions. AmirAli Nazari, et al considers DR and environmental uncertainty to allocate energy storage for a typical micro-grid and evaluate its economic value [24]. In addition, some researches consider demand response in long-term resource planning. For example, Andrew S, et al explore the analytical frameworks for incorporating DR into long-term resource planning[25]. Joao Anjo, et al assessed the impact of DR in the long-term by using a model of the Portuguese electricity system[26]. Ville O, et al assess the technical effectiveness of DR as a demand side flexibility option to mitigate variability in the energy system in Finland in 2030[27].

In comparison to existing research on planning and operation of IES where the determination of system capacity only considering the energy requirements, economy and operation conditions under different capacities without considering demand response, this study carries out a more rigorous analysis for planning and operation considering economy and environment and demand response. A generic optimal planning model is proposed to assess the economic and environmental benefits of the capacity allocation of the grid-connected IES considering demand response. The results of

three configuration modes are compared in the case study in detail, which shows the economic and environmental benefits brought by DR. In addition, the impact of sales capacity constraint to the grid and the fluctuations of electricity and gas prices on the allocation and operation of the IES are also studied considering PBDR.

The main contributions of the paper are summarized as follows:

- A generic optimal planning model is proposed to assess the economic and environmental benefits of the capacity allocation of the grid-connected IES considering demand response. The optimal planning problem is formulated as a mixed-integer linear programming model(MILP) with the objective to minimize the overall cost .
- DR is fully considered in the process of enconomic configuration of IES, which can avoid some of the new problems associated with implementing a DR strategy in a planned system, such as the massive curtailment of wind and solar. In this paper, the price-based demand response and incentive-based demand response are fully considered in the process of economic configuration of IES, respectively.
- Three different configuration modes are studied and compared to illustrate the economic and environmental benefits of demand response, and sensitivity analyses are performed to explore the impact of the sale capacity constraint and the fluctuation of electricity price and gas price on the planning and operation of IES.

The rest of the paper is organized as follows. An overview of the IES architecture and the basic planning optimal components model are presented in section 2. In Section 3, the demand response models are established. Section 4 proposes the optimal planning model including objective functions and constraints. Afterwards, numerical result and analysis are provided in Section 5. Finally, Section 6 concludes the paper.

2 Architecture of integrated energy system

IES is an integrated system containing energy production, supply and consumption, which can realize the coordination and optimization of different energy sources in energy system planning, construction, and operation. It is assumed that the system studied in this paper is always connected to the grid to ensure the energy balance of the system. When the energy supply of the system cannot meet the load demand or the excess energy within the system cannot be fully absorbed, the system will purchase electricity from the main grid or export the excess electricity to the grid and improve energy utilization efficiency. Fig. 1 is a typical overview architecture of IES.

As seen from Fig. 1, the components considered in IES include combined heating and power supply (CHP), wind turbine (WT), photovoltaic (PV), energy storage (battery storage, BAT) and power converter(COV). In addition, the main

end-users are divided into two categories: electrical load and heating load (hot water and space heating load). The electrical load is met by the grid, PV, WT, BAT and CHP, while the heating load is supplied by the recovery of waste heat from CHP and gas boiler (GB).

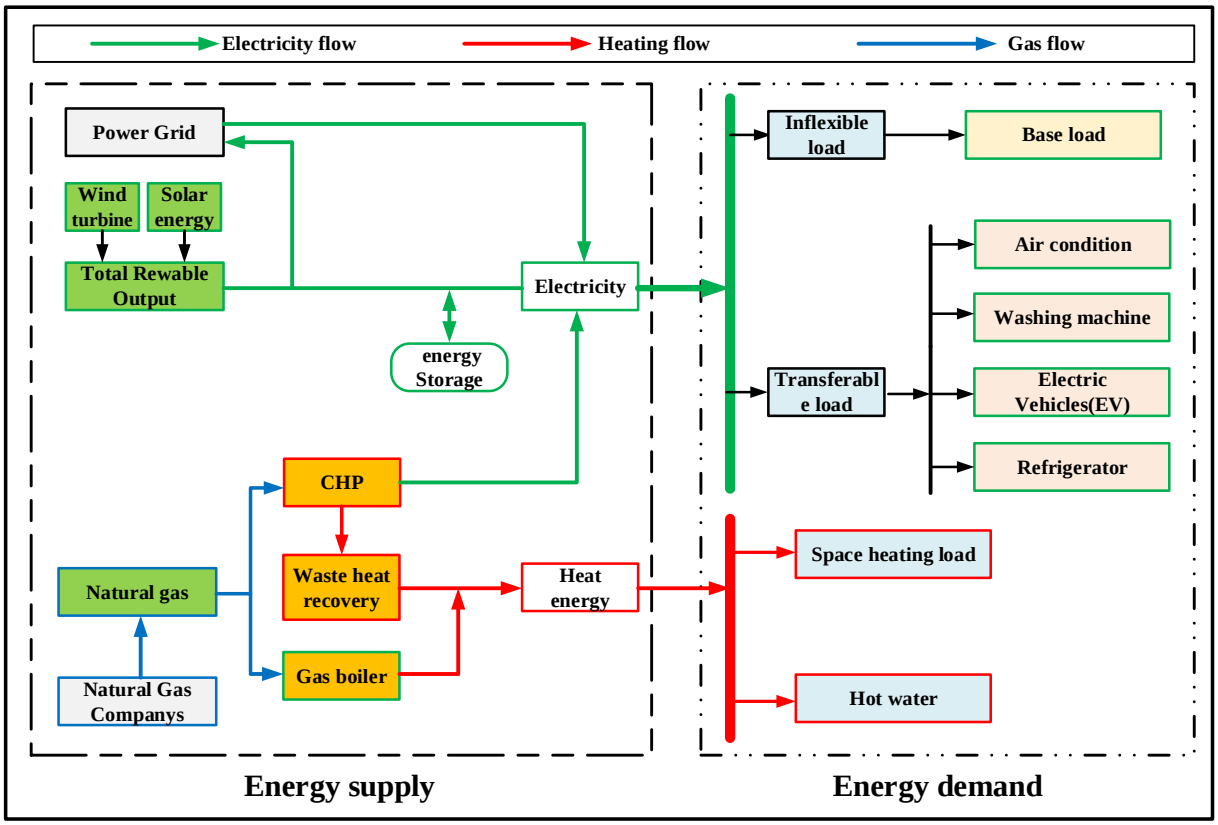

Fig. 1. Typical architecture of IES

2.1 Component models of integrated energy system

Fig. 1 shows a schematic of the proposed IES for this paper. The devices mainly include energy converters, renewables energy generators and storage devices and the following subsections model these components.

2.1.1 Solar photovoltaic

The actual output power of PV is determined by solar radiation and ambient temperature under standard test conditions(STC). The power output of the PV panels is calculated by (1):

$$P_{PV} = Y_{PV} f_{PV} \left(\frac{G_T}{G_{STC}} \right) [1 + \alpha_P (T_C - T_{STC})] \tag{1}$$

2.1.2 Wind turbine

The supplied power of wind turbines is calculated using a two-step procedure: (a) determining wind speeds at the hub height, (b) calculating the output power of WT. The relation between WT output and wind speed is formulated as:

$$P_{\mathrm{WT}}=\begin{cases}\bar{P}_{\mathrm{WT}}(v-v_{\mathrm{ci}})/(\bar{v}-v_{\mathrm{ci}}) & v_{\mathrm{ci}}\le v\le\bar{v}\\ \bar{P}_{\mathrm{WT}} & \bar{v}\le v\le v_{\mathrm{co}}\\ 0 & \text{else}\end{cases} \tag{2}$$

2.1.3 Power converter

A power converter is also an essential component in the hybrid renewable energy systems to convert DC power of PV panels and batteries to AC. The conversion efficiency for the converter is formulated as follows:

$$P_{t,\mathrm{out}}^{\mathrm{cov,AC}}=\eta^{\mathrm{cov}}P_{t,\mathrm{in}}^{\mathrm{cov,DC}} \tag{3}$$

2.1.4 Micro turbine

Micro turbine (MT) is the core device of CHP in this paper. When MT generates electricity, it will emit high-temperature flue gas as a by-production, which can supply the heating by recovering waste heat. Therefore, the cascade utilization of energy is realized, which can improve energy utilization and reduce polluted gas emissions. The fuel curve is used to illustrate the relationship between generator output and natural gas consumption as shown in Eq.(4)[28]. The relationship between heating and the electric power output is determined by the type of CHP turbine[29][30]. In this paper, the heat output is determined after determining the amount of power generation, the heat production of the CHP can be formulated as shown in Eq.(5).

$$F_t^{\mathrm{CHP}}=c_0Y_{\mathrm{MT}}+c_1P_t^{\mathrm{MT}} \tag{4}$$

$$Q_t^{\mathrm{CHP}}=\varsigma_{\mathrm{hr}}(\rho_{\mathrm{gas}}F_t^{\mathrm{CHP}}LHV_{\mathrm{gas}}-3.6P_t^{\mathrm{MT}})\Delta t \tag{5}$$

2.1.5 Battery

Given an intermittent renewable resource, such as solar and wind, accurate planning of electricity supply is a formidable task. Alternatively, batteries will assist scheduling of renewable energy systems by storing the electricity, maintaining a fixed voltage during the electrical load supply, and distributing the stored power with high efficiency. The energy storage model can be formulated as follows:

$$E^{t+1}=(1-\delta)E^{t}+(\eta^{c}P_t^{chg}-P_t^{dsg}/\eta^{d})\Delta t \tag{6}$$

2.1.6 Gas boiler

The gas boiler is used to fill the heat shortage when the waste heat is insufficient to meet the heat load demand. The relationship between boiler consumption of natural gas and its heat output is shown in Eq. (7).

$$Q_t^{\mathrm{boiler}}=\rho_{\mathrm{gas}}\eta_{\mathrm{boiler}}F_t^{\mathrm{boiler}}LHV_{\mathrm{gas}}\Delta t \tag{7}$$

3 Demand response modelling

In this paper, two types of demand response PBDR and IBDR are considered and the following subsections describe their modelling.

3.1 Price-based demand response model

PBDR is a no-cost demand response, and users spontaneously adjust power consumption based on electricity price. In this paper, the relationship between user electricity consumption and grid electricity price can be characterized by price elasticity. According to the stepwise elastic load curve modelling method in [31], this paper quotes 10 price points designed to express the relationship between an electricity price change and load change, thus obtaining the relationship between load response and incentive price. The load transfer rate can be determined according to the change rate of electricity price in *t* period. Then, the user load after the implementation of PBDR strategy is:

$$L_t^{pbdr} = L_t^{d0} \sum_{k \in K} \alpha_{kt} \eta_{kt} \tag{8}$$

$$\sum_{k \in K} \alpha_{kt} = 1, \alpha_{kt} \in \{0,1\} \tag{9}$$

$$\Delta L_t^{pbdr} = L_t^{pbdr} - L_t^{d0} \tag{10}$$

$$\left| \Delta L_t^{pbdr} \right| \le \Delta L_t^{pbdr,\max} \tag{11}$$

3.2 Incentive-based demand response modelling

In IES, there is often a large amount of curtailed wind and solar power due to that the energy cannot be fully absorbed by the power grid. Therefore, IBDR is implemented to absorb additional renewable energy in this paper. It is necessary to explain that the load involved in IBDR is only the electrical load. The electrical load in IES includes flexible load and inflexible load. In order to encourage users to participate in the IBDR, the operator needs to pay a certain amount of compensation to the user while ensuring the interests of the user.

According to Eq. (12), $L_t^{D0} \times \Delta L_t^{DR'}$ is related to flexible loads that participate in IBDR program. The term $L_t^{D0} \times \Delta L_t^{DR''}$ is related to the demand increase of flexible loads. At each *t* period, $\Delta L_t^{DR'} \le \Delta L_{\max}^{DR'}$ is used to ensure a high quality of living for users. In addition, the percentage of load increase ($\Delta L_t^{DR''}$)should be smaller than $\Delta L_{\max}^{DR''}$, and the sum of load reductions should be equal to the sum of load increments. If there is no customer participating in IBDR, $\Delta L_t^{DR'}$ =0 and $\Delta L_t^{DR''}$ =0, and the load has no change at period *t*. In this study, only 20% of base electric load participates in IBDR and 80% of each demand is considered to be inflexible[32].

$$L_t^{DR'}=L_t^{D0}(1-\Delta L_t^{DR'})+L_t^{D0}\times\Delta L_t^{DR''} \tag{12}$$

$$\sum_{t=1}^{T_d} L_t^{D0}\times\Delta L_t^{DR'}=\sum_{t=1}^{T_d} L_t^{D0}\times\Delta L_t^{DR''} \tag{13}$$

$$\Delta L_t^{DR'}\le\Delta L_{\max}^{DR'} \tag{14}$$

$$\Delta L_t^{DR''}\le\Delta L_{\max}^{DR''} \tag{15}$$

4. Optimal planning model of integrated energy system

The optimal planning model of IES is established based on the component model established in the previous section. The optimal planning model takes the minimum total annual planning cost of the system as the objective function, comprehensively considering the economic costs and environmental costs.

4.1. Objective function

The objective of the optimal allocation for the grid-connected IES is to minimize the total annual planning cost F_{tot}, containing the economic cost F_1 and environmental cost F_2.

$$F_{\text{tot}}=\min\{F_1+F_2\} \tag{16}$$

4.1.1 Economic cost

The economic cost consists of two parts, equipment acquisition cost $C_{\text{ann}}^{\text{EA}}$ and operating cost C_{OC} respectively.

$$F_1=C_{\text{ann}}^{\text{EA}}+C_{\text{OC}} \tag{17}$$

4.1.1.1 Equipment acquisition cost

It should be noted that the equipment purchase cost considered in this research is the acquisition cost under the whole life cycle, including initial investment costs, replacement cost, and equipment residual value at the end of the engineering project cycle. $C_{\text{ann}}^{\text{EA}}$ is the annual cost of equipment investment by averaging the total investment of equipment purchased during the whole life cycle. The annualized equipment acquisition cost is formulated as:

$$C_{\text{ann}}^{\text{EA}}=CRF(j,R_{\text{proj}})\sum_{i=1}^{M}\left[(a_i+b_i/j^{y_i})V_{\text{G},i}^{\text{cap}}-S_i\right] \tag{18}$$

$$CRF(j,R_{\text{proj}})=\frac{j(1+j)^{R_{\text{proj}}}}{(1+j)^{R_{\text{proj}}}-1} \tag{19}$$

4.1.1.2 Operation cost

Operation cost mainly includes three parts: (1) energy cost, which consists of electricity purchase cost, electricity sales revenue, and natural gas consumption cost; (2) operation and maintenance(O&M) of devices; (3) the compensation cost related to IBDR.

The operation cost is expressed as follows:

$$C_{\mathrm{OC}} = C_{\mathrm{grid,buy}} - C_{\mathrm{grid,sale}} + \sum_{t=1}^{T} C_t^{\mathrm{CHP}} + \sum_{t=1}^{T} C_t^{\mathrm{boiler}} + C_{\mathrm{op}}^{\mathrm{fixed}} + C_{\mathrm{IBDR}} \tag{20}$$

Eq. (23) and Eq. (24) are the natural gas consumption costs of CHP and GB in respectively. T is the total time slots in one year, which is 8760 in this paper.

$$C_{\mathrm{grid,buy}} = \sum_{t}^{T} c_t^{\mathrm{buy}} P_t^{\mathrm{buy}} \Delta t + \sum_{m=1}^{12} P_m^{\max} c^{\mathrm{demand}} \tag{21}$$

$$C_{\mathrm{grid,sale}} = \sum_{t}^{T} c_t^{sale} P_t^{\mathrm{sale}} \Delta t \tag{22}$$

$$C_t^{\mathrm{CHP}} = c^{\mathrm{gas}} F_t^{CHP} \Delta t \tag{23}$$

$$C_t^{\mathrm{boiler}} = c^{\mathrm{gas}} \frac{3.6 H_t \Delta t - Q_t^{\mathrm{CHP}}}{\rho_{\mathrm{gas}} LHV_{\mathrm{gas}} \eta_{\mathrm{boiler}}} \tag{24}$$

$$C_{\mathrm{op}}^{\mathrm{fixed}} = c_{\mathrm{pv}} V_{\mathrm{pv}}^{\mathrm{cap}} + c_{\mathrm{WT}} V_{\mathrm{WT}}^{\mathrm{cap}} + c_{\mathrm{bat}} V_{\mathrm{bat}}^{\mathrm{cap}} + c_{\mathrm{MT}} V_{\mathrm{MT}}^{\mathrm{cap}} t_{\mathrm{yr}} \tag{25}$$

$$C_{\mathrm{IBDR}} = \sum_{t=1}^{T} \lambda^{\mathrm{IBDR}} L_t^{\mathrm{D0}} \Delta L_t^{\mathrm{DR'}} \Delta t \tag{26}$$

4.1.2 Environmental cost

The environmental cost primarily is due to the emissions of pollutants from the upstream grid, CHP, and gas boiler. The emission gases considered in this paper mainly include carbon dioxide (CO_2), carbon monoxide(CO), nitrogen oxides(NO_x) and sulfur dioxide(SO_2). The environmental cost can be formulated as follows[33]:

$$F_2 = \min \left\{ \sum_{i=1}^{E} \pi^i \left\{ \sum_{t=1}^{T} d_{\mathrm{CHP}}^{\mathrm{gas},i} F_t^{CHP} \Delta t + \sum_{t=1}^{T} d_{\mathrm{boiler}}^{\mathrm{gas},i} F_t^{\mathrm{boiler}} \Delta t + \sum_{t=1}^{T} d_{grid}^{i} P_t^{\mathrm{buy}} \Delta t \right\} \right\} \tag{27}$$

4.2. Constraints

Constraints mainly include four categories: (1)equipment capacity constraint; (2)power constraints; (3) the operation constraints of storage battery; (4) the sale capacity constraint of the power grid; (5) the energy balance constraints.

4.2.1 Equipment capacity constraints

The installation size constraints for equipment capacity are as follows:

$$V_{G,i}^{cap,\min} \le V_{G,i}^{cap} \le V_{G,i}^{cap,\max} \tag{28}$$

4.2.2 Power constraints

In IES, the power of the equipment must remain within the maximum out power range considering the characteristics of the equipment and the safety and reliability requirements of the system.

$$\delta_i V_{G,i}^{cap} v_i^{\min} \le P_t^{\text{E-}i} \le \delta_i V_{G,i}^{cap} \tag{29}$$

Let $\xi_i=\delta_i V_{G,i}^{cap}$, then equation(29) can be linearized as:

$$\begin{cases} \xi_i v_i^{\min} \le P_t^{\text{E-}i} \le \xi_i \\ \delta_i V_{G,i}^{cap,\min} \le \xi_i \le \delta_i V_{G,i}^{cap,\max} \\ (1-\delta_i) V_G^{cap,\min} \le V_{G,i}^{cap} - \xi_i \le (1-\delta_i) V_G^{cap,\max} \end{cases} \tag{30}$$

4.2.3 Operation constraints of storage battery

The constraints of storage battery can be expressed as follows:

$$\begin{cases} 0 \le P_t^{\text{chg}} \le \delta_{chg} P_{\max}^{\text{bat}} \\ 0 \le P_t^{\text{dsg}} \le \delta_{\text{dsg}} P_{\max}^{\text{bat}} \\ \delta_{\text{dsg}} + \delta_{\text{chg}} = \{0,1\} \\ E^{\min} \le E^t \le E^{\max} \end{cases} \tag{31}$$

4.2.4. Sale capacity constraints

The sale capacity constraints is formulated as follows:

$$0 \le P_t^{\text{sale}} \le G^{\max} \tag{32}$$

4.2.5. Energy balance constraints

The IES should satisfy the energy balance, including electricity balance and heat balance. The energy balance can be formulated in Eq. (33) and Eq. (35). It is necessary to state that both the battery and the grid are considered to be load when the battery is charged and when excess power is sold to the grid.

$$\delta_{\text{buy}} P_t^{\text{buy}} + P_t^{\text{PV}} + P_t^{\text{WT}} + P_t^{\text{CHP}} + \delta_{\text{dsg}} P_t^{\text{dsg}} = \delta_{\text{chg}} P_t^{\text{chg}} + \delta_{\text{sale}} P_t^{\text{sale}} + L_t^{\text{d}} \tag{33}$$

$$\delta_{\text{buy}} + \delta_{\text{sale}} = \{0,1\} \tag{34}$$

$$H_t^{\text{CHP}} + H_t^{\text{GB}} = H_t^{\text{hotwater}} + H_t^{\text{spaceheating}} \tag{35}$$

5. Case study

An illustrative case study is designated for a chosen region to verify the reliability and rationality of the proposed capacity planning and optimization model. According to the wind speed, light intensity, temperature, and load demand of the community, the optimization model proposed in this paper is used for capacity planning and optimization. The proposed planning model is programed and solved through MATLAB optimization toolbox.

5.1 Parameters

The input parameters used in the simulation mainly include equipment capacity, unit power investment and O&M cost, as well as load curve, energy price and emission, etc. Fig. 2 and Fig. 3 show the wind speed and solar intensity. Fig. 4 and Fig. 5 show the annual electric load and thermal load of the district, respectively. The data of typical daily power and thermal loads in summer and winter are shown in Fig. 6. The basic technical parameters of equipment purchased are shown in Tab. 1. The energy price in each period is shown in Table 2. In addition, the sale capacity is no more than 300kW considering the safety of the grid.

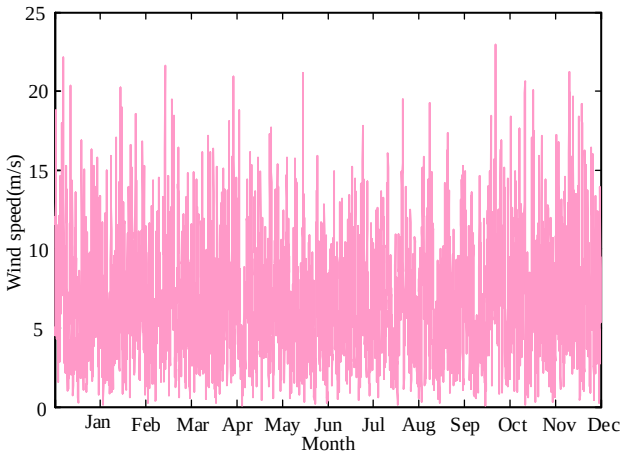

Fig. 2. Annual wind speed

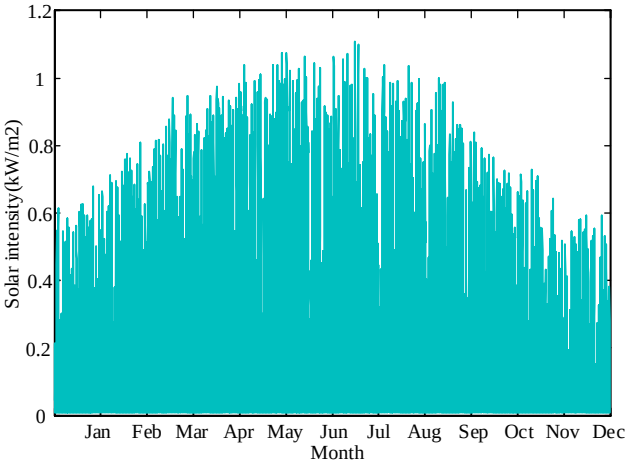

Fig. 3. Annual solar intensity

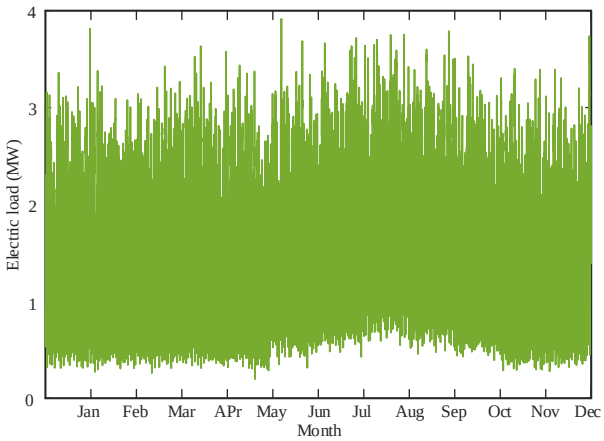

Fig. 4. Annual electric load

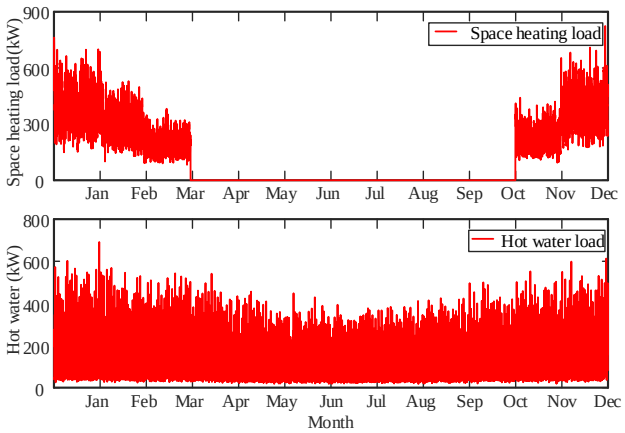

Fig. 5. Yearly space heating load and hot water load

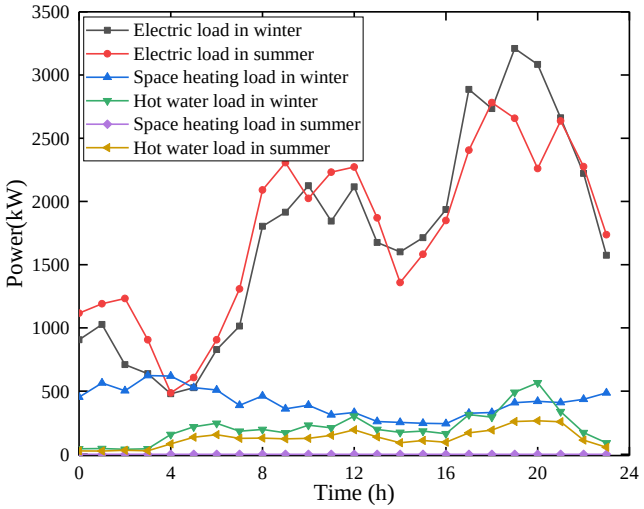

Fig. 6. Electric and thermal load curve on a typical day in winter and summer

Table 1 Technology parameters of the components

Device type	capacity	Investment	Replacement	O&M	Technical lifetime
PV	1kW	3400yuan/kW	3400yuan/kW	100yuan/yr	25 yrs
WT	1kW	5000yuan/kW	5000yuan/kW	50yuan/yr	20yrs
MT	1kW	2000yuan/kW	2000yuan/kW	0.02yuan/h	40000h
BAT	1kWh	1250yuan/kWh	1250yuan/kWh	100yuan/yr	10yrs
COV	1kW	1000yuan/kW	1000yuan/kW	50yuan/yr	15yrs

Table 2 The market energy price of IES

Energy price types	Time interval	Value
NG price	0:00-23:00	2.9 (yuan/m³)
Electricity price	23:00-6:00	0.402 (yuan/kWh)
	7:00-9:00;13:00-17:00	0.614 (yuan/kWh)
	10：00-12:00;18:00-22:00	0.925 (yuan/kWh)
sale price	23:00-6:00	0.2 (yuan/kWh)
	7:00-9:00;13:00-17:00	0.3 (yuan/kWh)
	10：00-12:00;18:00-22:00	0.4 (yuan/kWh)
compensation price	——	0.65(yuan/kWh)

5.2. Results and discussions

In this section, three DR modes are built for comparative analysis to explore the impact of different DR schemes on planning and optimization in the community energy system.

Mode1: Demand response is not considered in planning, which is the reference model.

Mode2: PBDR is considered in planning and operation.

Mode3: IBDR is considered in planning and operation.

5.2.1 Effect of demand response on the load curve

Because the climate change in the spring and autumn is not obvious in this area, the typical daily load curves in summer and winter are adopted to illustrate the effect of PBDR and IBDR. As seen from Fig. 7~8, based on electricity price signals, a part of the load is transferred from the peak period to the flat and valley periods. Fig. 9 and Fig. 10 show the implementation effect on IBDR. It can be seen that a part of loads is transferred from the night into daytime when the PV output is sufficient. The load curve is smoothed after implementing IBDR.

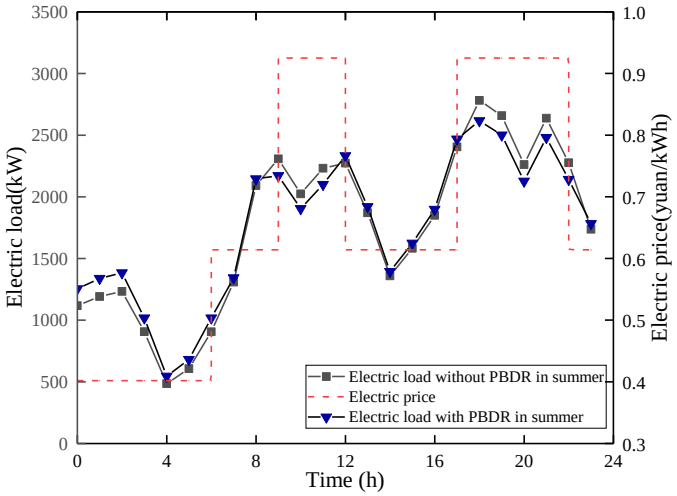

Fig. 7. Electric load with and without PBDR in summer

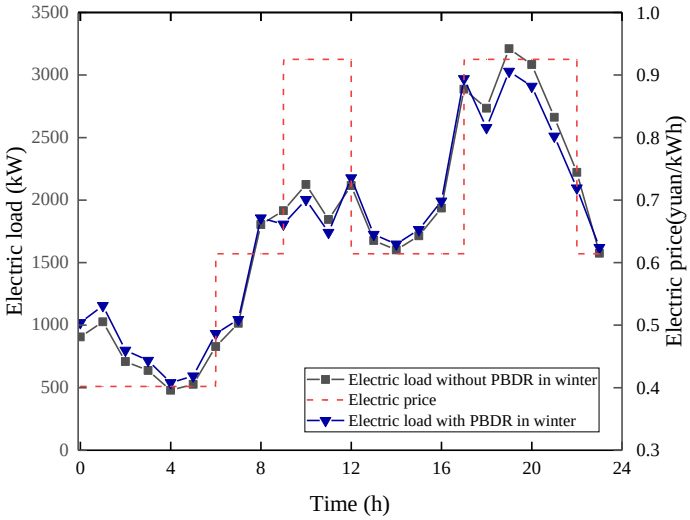

Fig. 8. Electric load with and without PBDR in winter

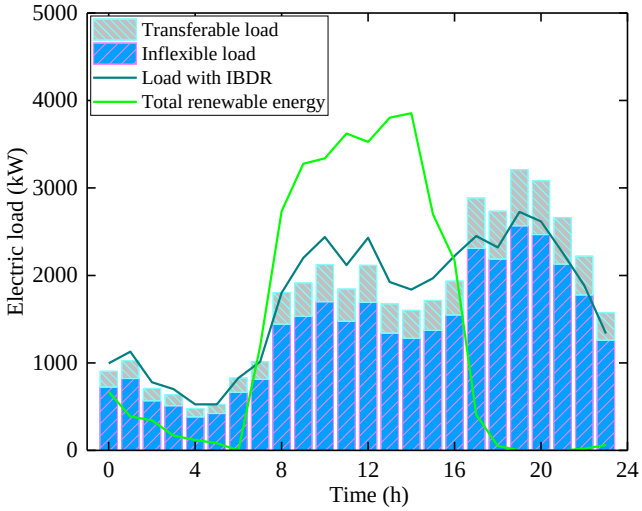

Fig. 9. IBDR implementation effect on a typical day in winter

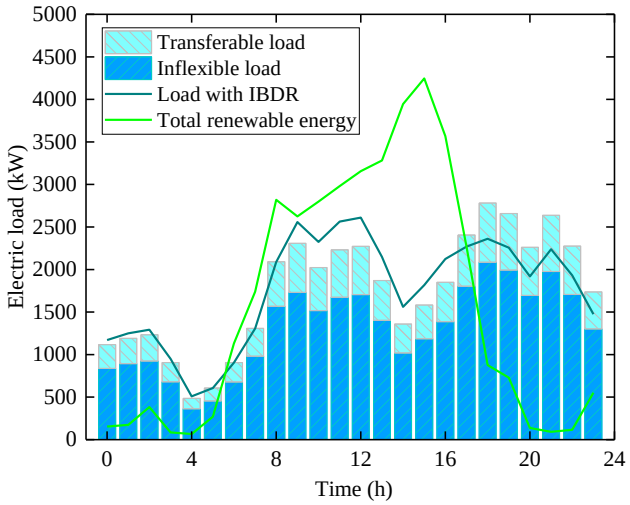

Fig. 10. IBDR implementation effect on a typical day in summer

5.2.2 Optimal planning results

The configuration results of 3 modes are shown in Table 3. As shown from Table. 3, compared with M1, in M2, the economic cost is reduced by 0.114 million yuan, and the environmental cost is reduced by 0.115 million yuan, which are reduced by 1.17% and 5.024%, respectively. It can be seen that the benefits of PBDR are more reflected in environmental protection. From the perspective of the configuration capacity of each device, the capacity of PV has increased by 129kW, and the capacity of WT has reduced by 30 kW, while the total renewable installed capacity has increased 99kW. Meanwhile, the capacity of energy storage has dramatically increased by 976 kWh, while the capacity of CHP has reduced by 20kW. In general, the overall economic and environmental benefits are higher than M1. The cost analysis can be found in sections 5.2.3 and 5.2.4.

Likewise, compared with M1, the capacity of PV has increased by 491kW in mode3(M3), and the capacity of WT has reduced by 330kW, while the total renewable energy installed capacity has increased by 161kW. Moreover, the capacity of the battery has reduced by 200kWh and the CHP's capacity does not change. It can be concluded that the IBDR strategy helps reduce the installed capacity of the storage battery. In addition, both economic cost and environmental cost have small reductions, which decrease by 7.34% and 7.99%, respectively. Overall, M3 has the lowest total planning cost.

Table 3 Comparison of the cost-optimal configuration of integrated energy system in three modes

Modes	PV(kW)	WT(kW)	BAT(kWh)	COV(KW)	CHP(kW)	F1(million yuan)	F2(million yuan)	CDR(million yuan)	F_{tot}(million yuan)
M1	3000	4000	1094	2034	380	9.8093	2.289	0	12.0983
M2	3129	3970	2070	1951	360	9.6953	2.174	0	11.8693
M3	3491	3670	894	2368	380	9.0893	2.106	0.634	11.8293

5.2.3 Investment cost analysis

To better compare the economic impacts of demand response, Fig. 11~13 display the cost broken down by components and types for the three modes. According to Fig. 11~13, the battery and WT have the highest replacement costs, respectively. The lifespan of PV is equal to the project engineering cycle. There is no replacement cost for PV and the wind turbine needs to be replaced in the 20th year. The WT account for a large proportion in terms of residual value. The value of the WT replacement has not been fully utilized, which indicates that the installation benefits of PV is better than that of wind power. Moreover, the battery is replaced twice during the life of the project so the installed capacity of the battery cannot be too large. In addition, as seen from Fig. 11~13, the converter has a certain proportion in the initial investment cost and replacement cost. The proportion of COV in the initial investment cost of three modes are 5.92%, 5.46%, 6.87%, and that in replacement costs are 9.35%, 8.4%, and 11.67%, respectively . So it is necessary to consider the converter in the planning.

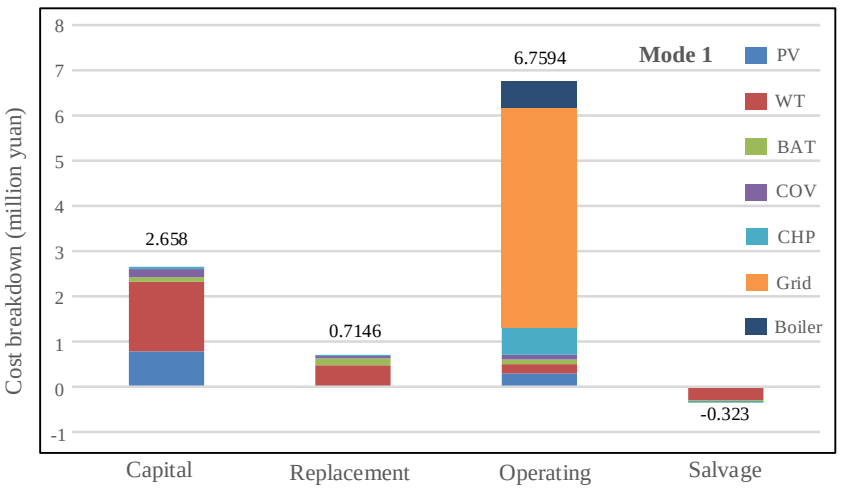

Fig. 11. Costs breakdown by components and types (mode 1)

When comparing the three modes in terms of different cost types, the operating cost is the most considerable. Among the operating costs, it is mainly the cost of purchasing electricity and the cost of purchasing gas. The purchase cost on the grid side accounts for a large part. As shown in Fig. 11~13, the three modes have relatively similar costs for different parts of the system. However, compared with mode 1, the initial investment cost of the system (mode 2) with PBDR is increased by 0.107 million, but the total annual operating cost decreases by 0.2826 million. The operating cost of the configuration system in mode 3 is the minimum in all modes. Compared to Mode 1, the initial investment cost of mode 3 is slightly increased.

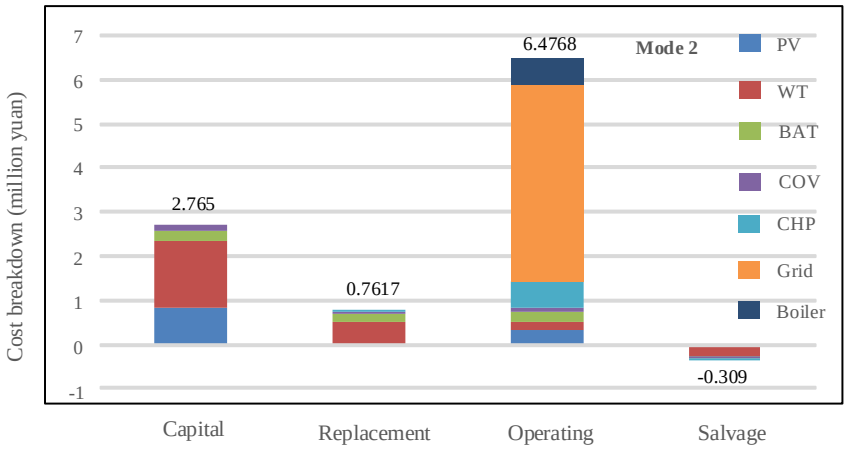

Fig. 12. Costs breakdown by components and types (mode 2)

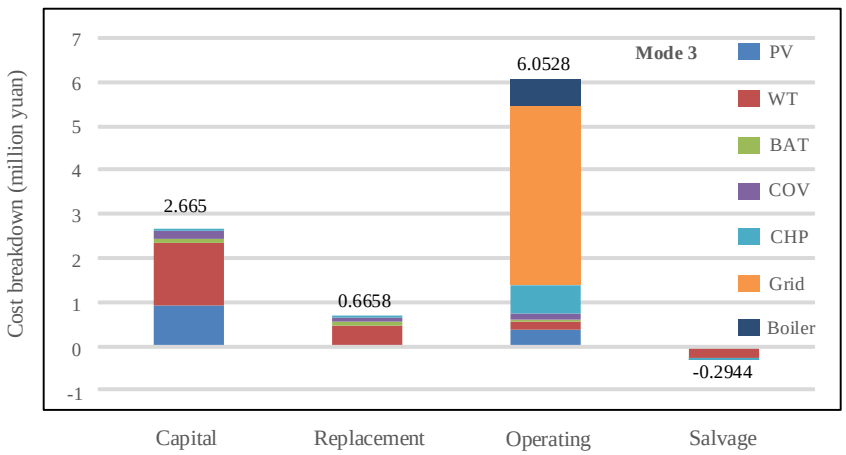

Fig. 13. Costs breakdwon by components and types (mode 3)

5.2.4 Operation cost decomposition analysis

According to the planning model, the operating costs involved include electricity purchase cost, fuel cost, O&M cost, and etc. Some operation costs components of different modes are shown in Table 4. In order to explain the problem more clearly, the environmental costs are also compared.

Table 4 Operation costs of different modes

Modes	Power demand cost(million yuan)	Fuel cost (million yuan)	Electricity purchase cost(million yuan)	Electricity sale Revenue(million yuan)	Environmental cost(million yuan)	IBDR cost (million yuan)
M1	1.73	1.194	3.412	-0.305	2.289	0
M2	1.625	1.181	3.127	-0.456	2.174	0
M3	1.442	1.196	2.971	-0.313	2.106	0.634

Fig. 14 illustrates the cost composition under different configuration modes in detail. It is clear that the proportion of electricity purchase cost is the largest in all types of costs and its value has a certain reduction under the configuration system considering demand response (M2 and M3). Meanwhile, both the power demand cost and the environmental cost have decreased in M2 and M3. As can be seen from Table 4, compared with M1, the power demand costs of M2 and M3 are reduced by 6.07% and 16.65%, respectively. Likewise, the environmental cost of M2 and M3 are reduced by 5.02% and 7.99%, respectively.

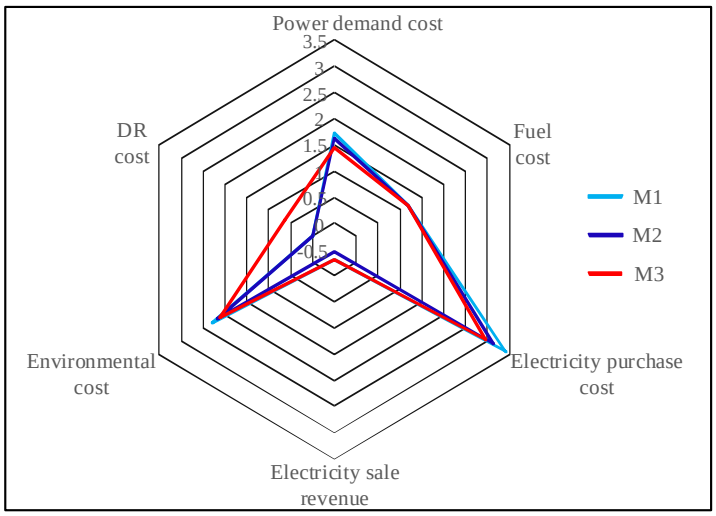

Fig. 14. Operation cost composition with different modes

5.2.5. Operation optimization simulation

In order to further study the operation of IES under different modes, two typical operating days are selected for analysis. The output and operation state of each part of the configuration system are shown in Figs. 15-18.

The electric load and the output of the power supply module in M1~M3 are shown in Fig. 15. The thermal load and the output of the thermal supply module in M1~M3 are shown in Fig. 16, Fig. 17, Fig. 18, respectively. As seen from Fig.15, the output and operation optimization of the total renewable energy (PV and WT) have similar trends in three modes, which are greatly influenced by the installed equipment capacity and weather factors.

From the operating state of the three modes, the energy storage battery will be charged only when the total renewable

energy generation is greater than the load demand whether in winter or summer at any time period *t*, and the battery is only charged by renewable energy. When the total output of renewable energy is less than the load demand, it is preferentially supplied through the discharge of the energy storage battery, and the minimum state of charge(SOC) of the battery is not less than 20%. For the power interaction between the system and the grid, the premise that the system can sell electricity to the grid is that the renewable energy is sufficient, and the energy storage battery is not enough to absorb surplus renewable energy. Moreover, considering the stable operation of the power grid, the power sold by the system to the grid is constrained to 300 kW. In some periods, surplus renewable energy cannot flow into the grid, which will cause a certain amount of energy waste. The impact of the constraint of power flowing into the grid on system planning will be discussed in Section 5.2.6.1.

In addition, the operating state of CHP is more affected by seasonality. The main reason is that the heating load demand in winter and summer is inconsistent. From the operation of three modes, it can be seen that there is no space heating load in the summer, and the heat demand is mainly the hot water load. The CHP has a short operating time and mainly concentrated during the night load peak period. In the winter, due to the space heating load demand, the ratio of electric load to heating load is reduced, and the profit of running CHP is large at this time.

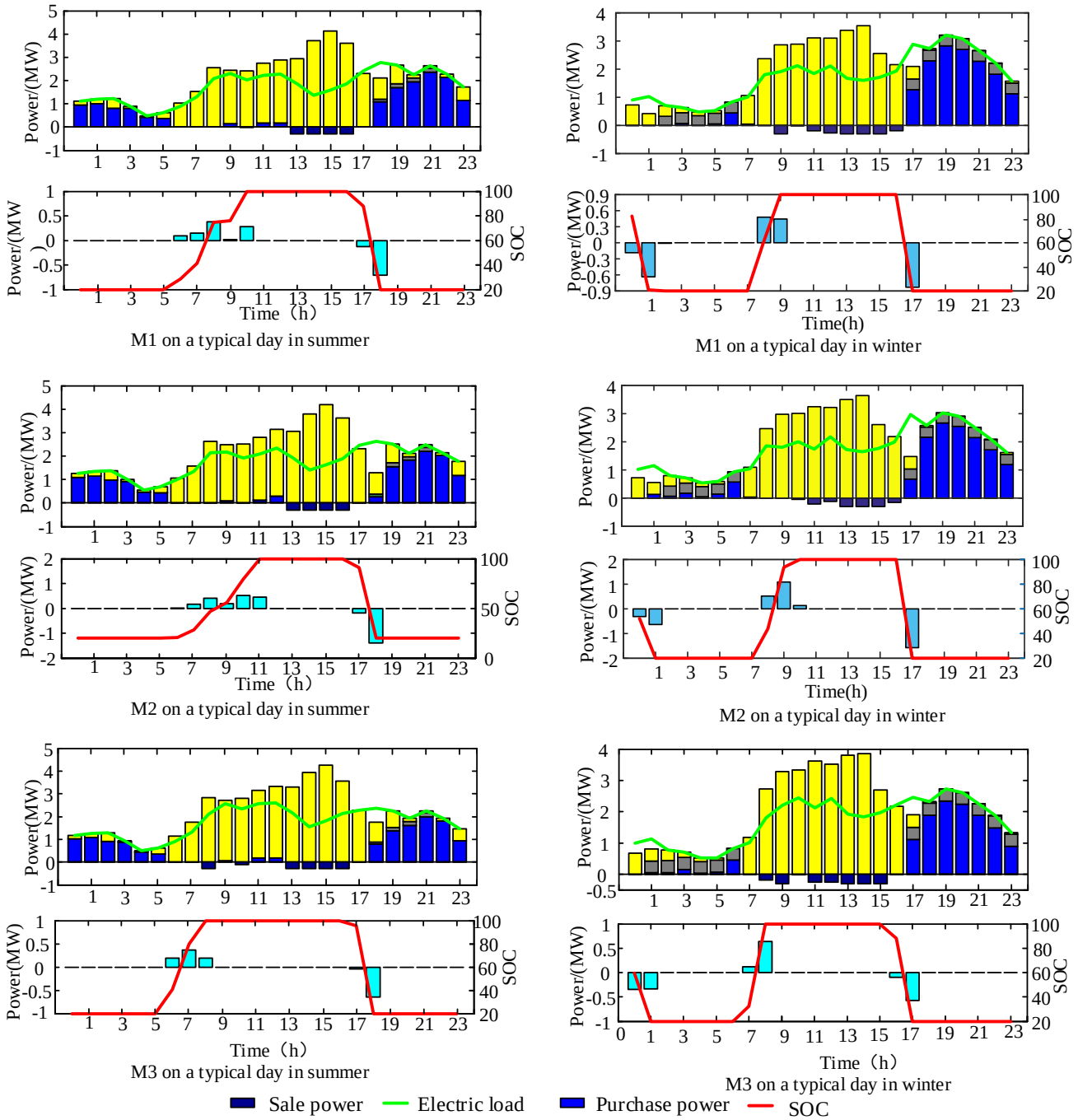

Fig. 15 Electric load operation of three modes on a typical day in winter and summer

For the operation of the heat load, it can be seen that the supply of heat load is supplied by the CHP and the gas boiler, and the CHP unit has the priority of heating. The gas boiler is combined with the CHP unit for differential replenishment. In addition, as mentioned above, the CHP unit operates in a "heat-fixing" mode, and its heat production is limited by the amount of power generated. In the winter, the cascade utilization of energy is greatly realized due to the waste heat recovery and utilization of the CHP unit, and the cost of purchasing electricity and the cost of purchasing gas are reduced.

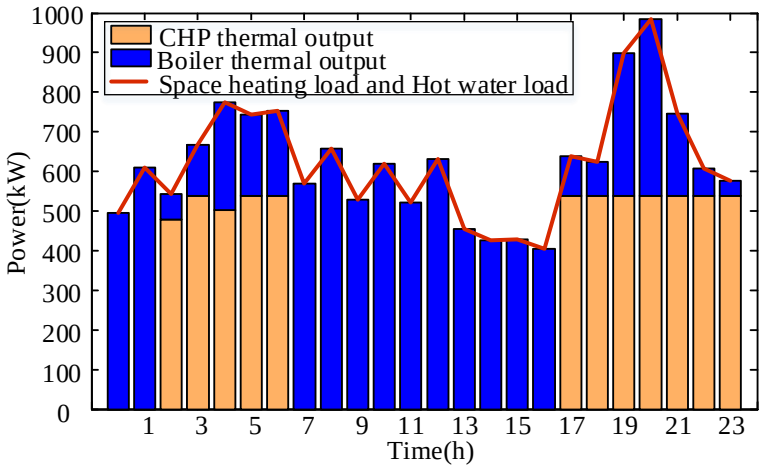

Fig. 16(a). Thermal load operation of mode 1 on a typical day in winter

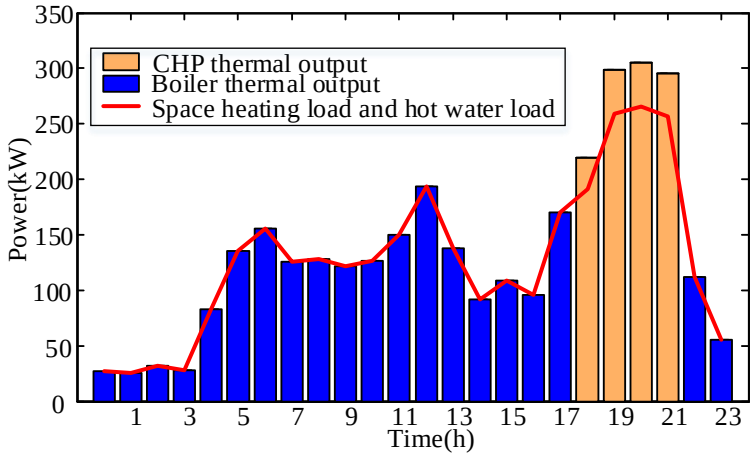

Fig. 16(b). Thermal load operation of mode 1 on a typical day in summer

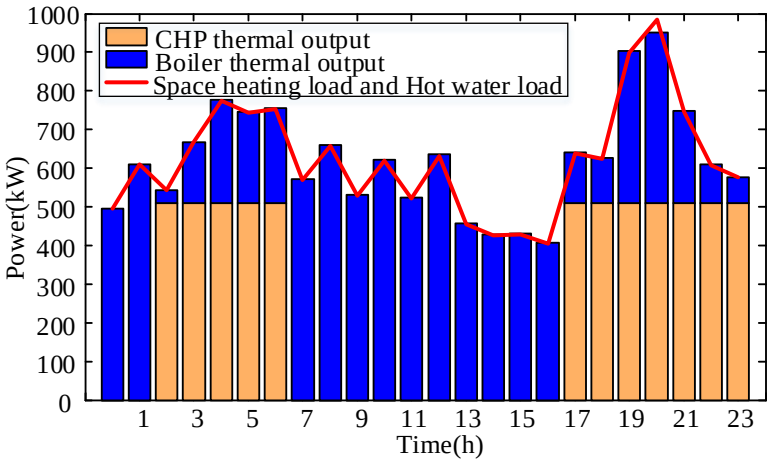

Fig. 17(a). Thermal load operation of mode 2 on a typical day in winter

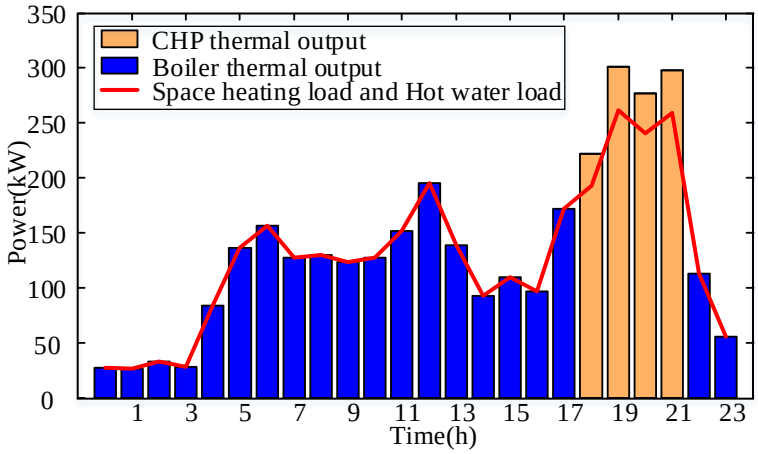

Fig. 17(b). Thermal load operation of mode 2 on a typical day in summer

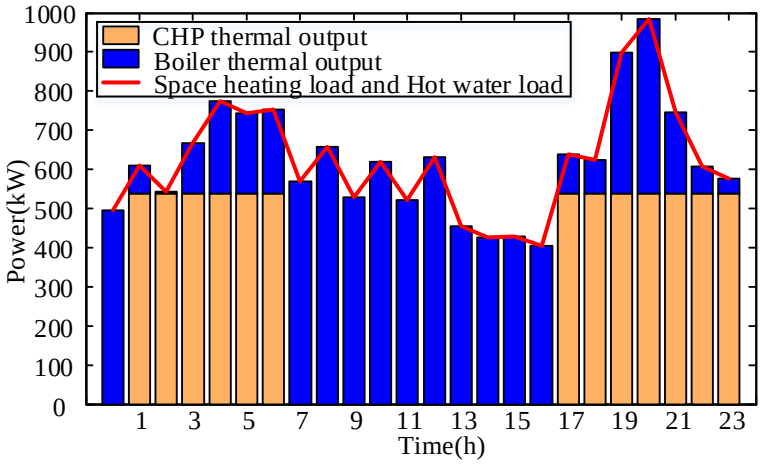

Fig. 18(a). Thermal load operation of mode 3 on a typical day in winter

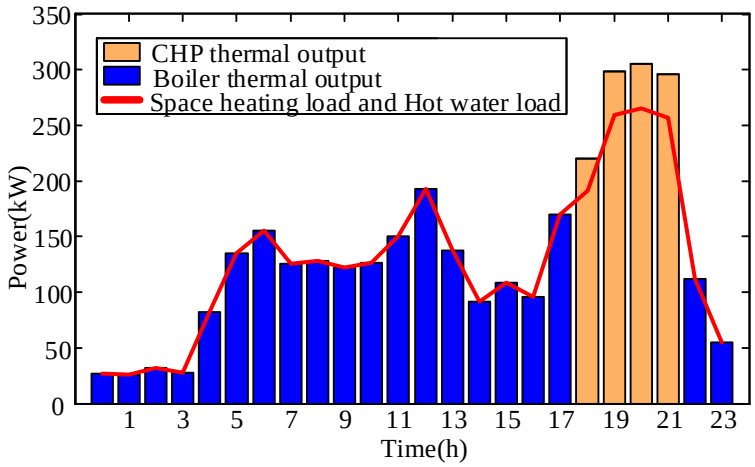

Fig. 18(b). Thermal load operation of mode 3 on a typical day in summer

5.2.6 Sensitivity analysis of key parameters

The impacts of the external parameters on the planning results of the IES are investigated as follows.

5.2.6.1 Sale constraint sensitivity analysis

In the actual planning, the power of the IES to sell electricity to the grid has an upper limit to ensure the safety and stability of the grid operation. This section explores the impact of different sale constraints on the configuration and operational results in M2. Table.5 shows the results of sensitivity analysis under different power sales constraints.

Table 5 Sensitivity analysis results under different sale capacity constraints

sale constraint(kW)	PV(kW)	WT(kW)	Total Renewable(kW)	CHP(kW)	BAT(kWh)	COV(kW)	F1(million yuan)	F2(million yuan)	Excess electicity(%)
0	3029	3920	6949	400	3270	1880	10.041	2.094	28.80%
100	3100	4020	7120	390	3408	1871	9.989	2.056	28.40%
200	3078	4100	7178	390	3376	1861	9.908	2.049	27.60%
300	3129	3970	7099	390	2070	1951	9.695	2.174	26.60%
400	3044	4040	7084	420	2208	1955	9.615	2.167	25.20%
500	3125	4170	7295	390	2182	2008	9.557	2.137	25.20%
600	3173	4010	7183	380	514	2104	9.278	2.325	24%
700	3181	4100	7281	380	490	2124	9.211	2.314	23.30%
800	3218	4350	7568	390	368	2129	9.135	2.293	23.90%
900	3237	4350	7587	390	100	2252	9.013	2.331	22.70%

It can be seen from Table 5 that with the increase of power sales constraints, the installed capacity of PV and WT generally show an increasing trend. At the same time, the number of converter device has increased as the increase of installed capacity of PV. Conversely, the capacity of the energy storage battery is significantly reduced with the increase of power sale constraints, while the installed capacity of the CHP unit is not significantly changed. It can be concluded that the optimal installed capacity of the energy storage battery is most sensitive to the power sale constraints.

In addition, Fig. 19 illustrates the trend of the economic cost, environmental cost, and the amount of excess electricity with different sale constraints in detail. It is worth mentioning that the value of parameters in Fig. 19 are per unit values, and their maximum is taken as the base value. It is seen from Fig. 19 that the economic cost and the amount of excess electricity have a downward trend with the increase in sale constraint. Conversely, the environmental cost shows the trend of increasing step by step, and there is a slow downward trend at each step. It can be concluded that the decrease in energy storage capacity caused by the increase in power sales constraints leads to an increase in environmental costs. In other words, the installation of energy storage is beneficial to energy conservation and emission reduction, while reducing the cost of emission penalties.

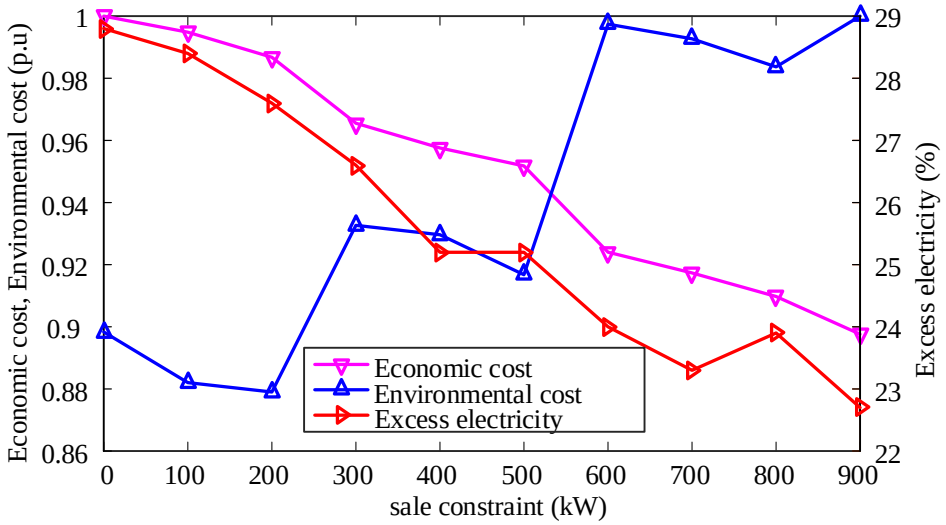

Fig. 19. Results of sensitivity analysis with different sale constraints

Based on the above analysis, it can be concluded that the power interaction between the power grid and the IES is not only related to the stable operation of the power grid, the reasonable determination of the sale capacity constraint is also conducive to improving the energy saving and emission reduction benefits of IES.

5.2.6.2 Gas price sensitivity analysis

Table. 6 shows the results of sensitivity analysis under different natural gas prices.

Table 6 Configuration and operation results with different natural gas prices

Natural gas price (yuan/m^3)	PV(kW)	WT(kW)	Total Renewable(kW)	CHP(kW)	BAT(kWh)	COV(kW)	CHP operating time(h)	Electricity purchase cost(million yuan)	Natural gas purchase(m^3)	F1(million yuan)	F2(million yuan)
1.00	2978	3870	6848	390	1274	1985	2763	4.565	446019	8.775	2.268
1.50	3063	3920	6983	390	1274	1932	2559	4.551	438369	9.019	2.253
2.00	3053	3950	7003	390	2090	1890	2306	4.448	423965	9.317	2.176
2.50	3044	3960	7004	380	2202	1895	2153	4.452	414738	9.535	2.170
2.90	3129	3970	7099	360	2070	1951	1994	4.466	407135	9.695	2.174
3.50	3139	4050	7189	370	3284	1891	1369	4.328	376431	10.021	2.085
4.00	3036	4120	7156	370	2824	1953	1238	4.451	363822	10.172	2.133
4.50	3212	4100	7312	320	3542	1932	1052	4.361	350511	10.424	2.064
5.00	3216	4200	7416	320	3520	1916	804	4.369	343359	10.783	2.057

It is clear from Table 6 that there are significant differences in capacity configurations and operations under the different natural gas price. However, the trend of data changes is not obvious. Fig. 20 illustrates the trend of some data in Table 6 in detail. Likewise, the value of parameters in Fig. 20 are per unit values based on the results of mode 2.

It can be seen from Fig. 20 that the increasing natural gas price leads to a decrease in the operational efficiency of CHP, which leads to a decline in natural gas consumption. Thus the economy can be optimized by reducing the capacity of the

CHP unit. It reflects that the price change of natural gas has a great impact on the operation of the system with large capacity CHP. Moreover, as seen from Table 6, with increasing gas price, the installed capacity of renewable energy generation rises, but the total capacity increase is not very large due to the sales capacity constraint and zero output of PV at night. However, a significant increase in storage capacity has resulted in lower purchases and lower environmental costs. In addition, the annual average planning cost increases almost linearly with rising gas prices. According to the analysis, when the price of natural gas increases, the economic and environmental benefits produced by increasing the installed capacity of energy storage are the best.

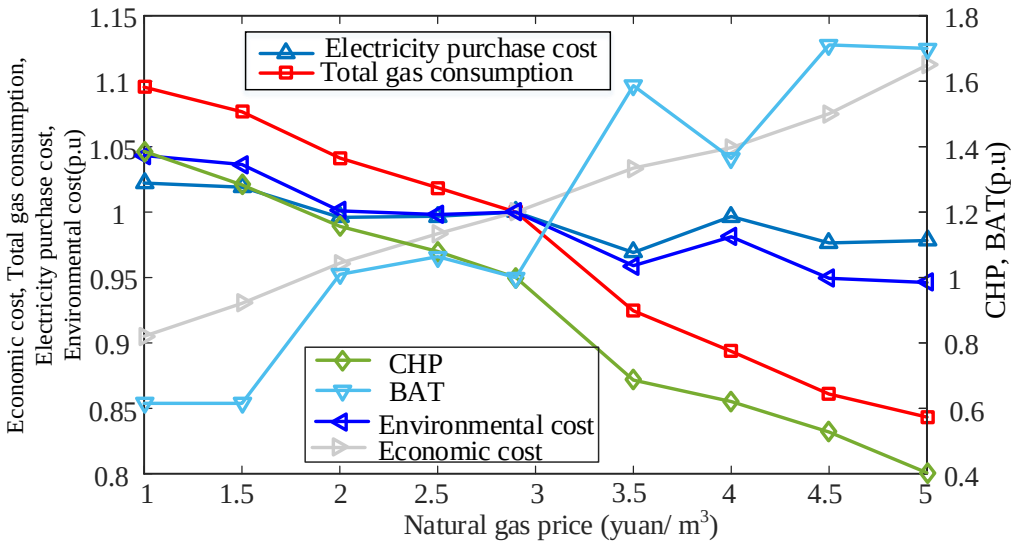

Fig. 20. Results of sensitivity analysis with different natural gas price

5.2.6.3 Electricity price sensitivity analysis

The price of the electricity price in the market is also fluctuating. The work in this section mainly studies the impact of the different electricity price (±2%、±5%、±7%、±10%) on system configuration under the condition of M2. Table. 7 shows the results of sensitivity analysis under different electricity price.

Table 7 Configuration and operation results with different natural gas prices

Electricity price	PV(kW)	WT(kW)	Total Renewable(kW)	CHP(kW)	BAT(kWh)	COV(kW)	Electricity purchase (kWh)	Natural gas purchase(m^3)	F1(million yuan)	F2(million yuan)
-10%	2931	3740	6671	360	394	1952	4809535	410238.8	9.114	2.427
-7%	3082	3780	6862	370	622	1982	4666662	410577.8	9.276	2.368
-5%	3042	3960	7002	390	1376	1958	4426743	404966.8	9.448	2.261
-2%	3066	3940	7006	420	2186	1921	4251670	402954.9	9.621	2.186
0	3129	3970	7099	360	2070	1951	4238243	407135.2	9.695	2.174
2%	3215	4130	7345	430	3526	1880	3857006	399491.2	9.914	2.017
5%	3186	4330	7516	370	3718	1858	3733951	400875.3	10.047	1.967
7%	3179	4340	7519	390	3762	1868	3720703	401473.2	10.107	1.962
10%	3273	4350	7623	420	4190	1826	3614115	401206.1	10.234	1.918

It is clear from Fig. 21 that the fluctuation of electricity price has the greatest impact on the installed capacity of energy storage, which increases dramatically with the increase in electricity price. However, the installed capacity of total renewable energy increases slightly with the increase of electricity price due to the sale capacity constraints. At the same time, the annual total planning cost increases almost linearly. In addition, both the quantity of electricity purchased and the environmental cost have been significantly reduced with the increase in electricity price. It can be concluded that the economic and environmental benefits brought by increasing the capacity of energy storage, when electricity prices increase, are also optimal, and the appropriate increase in electricity price, while increasing planning costs, can reduce emissions of polluting gases and increase environmental benefits.

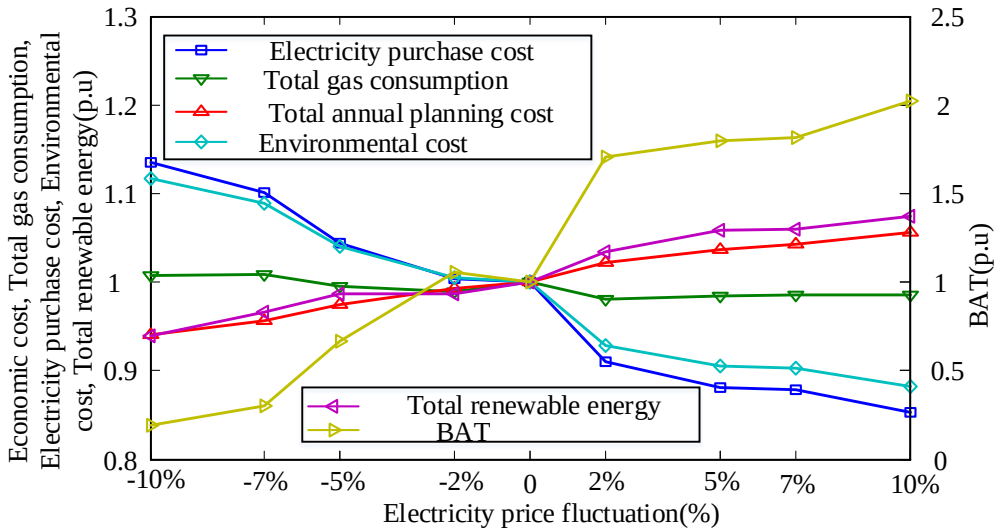

Fig. 21 Results of sensitivity analysis with different electricity prices

6 Conclusion

A generic optimal planning framework and model is proposed to assess the economic and environmental benefits of the capacity allocation of the grid-connected integrated energy system considering both price-based demand response and incentive-based demand response respectively. The optimal planning problem is formulated as a mixed-integer linear programming model with the objective to minimize the total annual cost including the economic cost and environmental cost. In the case simulation, three configuration modes are studied to illustrate the economic and environmental benefits of demand response. Mode1 is reference mode, which does not consider DR in planning of IES. Mode2 and mode3 consider PBDR and INDR in planning of IES, respectively. Simulation results show that the mode2 and mode3 show better economic and environmental benefits than mode1. Through the cost-benefit analysis, compared with mode 1, the investment costs of mode 2 and mode 3 increased by 4.03% and 0.26%, respectively, while the operating costs of mode 2 and mode 3 decreased by 4.18% and 10.45%, respectively. It can be found that the initial investment cost of the equipment is slightly increased, but the operating cost is greatly reduced. The difference in operating costs is mainly reflected in the power demand cost and the cost of purchasing electricity. Compared with mode 1, the power demand cost of mode 2 and mode 3 is reduced by 6.07% and 16.65%, respectively, and electricity purchase cost of mode 2 and mode 3 reduced by 8.35% and 12.93%, respectively. Compared with mode1, the economic and environmental costs of mode2 decreased by 1.17% and 5.024%, respectively, and the economic and environmental costs of mode3 decreased by 7.34% and 7.99%, respectively. Overall, mode3 has the lowest total planning cost.

In addition, the influence of the sales capacity constraint to the grid and the fluctuation of electricity price and gas price on the planning of the IES are explored under the condition of mode 2. The sensitivity analysis results can be summarized as follows:

(1) The sales capacity constraint has a great influence on the consumption rate of renewable energy and the installed capacity of energy storage. Under the premise of ensuring the safe and stable operation of the power grid, appropriately increasing the size of the sales capacity can reduce the investment in energy storage and increase the utilization rate of renewable energy.

(2) Through the sensitivity analysis of gas price, it can be found that the change of gas price has great influence on the operation of CHP unit. The increase of gas price, the optimal installed capacity of CHP unit shows a downward trend, and the operating efficiency of CHP unit is significantly reduced. It can be conclude that the price change of natural gas has a great impact on the operation of the system with large capacity CHP.

(3) The fluctuation of electricity price has the greatest impact on the installed capacity of energy storage, which increases dramatically with the increase in electricity price. In addition, both the quantity of electricity purchased and the environmental cost have been significantly reduced with the increase in electricity price. It can be concluded that the economic and environmental benefits brought by increasing the capacity of energy storage, when electricity prices increase, are optimal, and the appropriate increase in electricity price, while increasing planning costs, can reduce emissions of polluting gases and increase environmental benefits.

Acknowledgement

This work was supported by the National Natural Science Foundation of China (51807127), the Sichuan Science and Technology Program (2019YFH0171), Young Elite Scientists Sponsorship Program By CSEE (CSEE-YESS-2018006), and International Visiting Program for Excellent Young Scholars of Sichuan University.

References

[1] Bowen Hong, Weitong Zhang, Yue Zhou, et al. Energy-Internet-oriented microgrid energy management system architecture and its application in China. Applied Energy 2018, 228:2153-2164.

[2] Xiaodan Yu, Xiangdong Xu, Shuoyi Chen, et al. A brief review to integrated energy system and energy internet. Trans China Electrotech Soc 2016;31(1):1-13.

[3] ZHAO Shan, WEN Lixing, ZHAO W ei, et al. Power quality research based on micro power grid. Guangdong Electr Power Syst 2012;25(10):61e4.

[4] Chao Qin, Qingyou Yan, Gang He, Integrated Energy Systems Planning with Electricity, Heat and Gas Using Particle Swarm Optimization, Energy (2019), https://doi.org/10.1016/j.energy.2019.116044

[5] Yang Y, Zhang S, Xiao Y. An MILP (mixed integer linear programming) model for optimal design of district-scale distributed energy resource systems. Energy 2015;90:1901e15.

[6] Quashie M, Marnay C, Bouffard F, et al. Optimal planning of microgrid power and operating reserve capacity. Appl Energy 2018:210.

[7] Jaesung J, Michael V. Optimal planning and design of hybrid renewable energy systems for microgrids. Renewable and Sustainable Energy Reviews 2017; 75: 180-191.

[8] Patrizia S, Gioacchino N, Gellio C. Planning and design of sustainable smart multi energy systems. The case of a food industrial district in Italy. Energy 2018; 163:443-456.

[9] Tengfei Ma, Junyong Wu, Liangliang Hao, et al. The optimal structure planning and energy management strategies of smart multi energy system. Energy 2018; 160: 122-141.

[10] Xing Yan, Yusuf Ozturk, Zechun Hu, et al. A review on price-driven residential demand response. Renewzble and Sustainable Energy Reviews 2018;96:411-419.

[11] Danielly B. Avancini, Joel J. P .C. Rodrigues, Simion G. B. Martins, et al. Energy meters evolution in smart grid:

A review. Journal of Cleaner Production 2019;217:702-715.

[12] Luis I. Minchala-Avila, Jairo Armojos, Daniel Pesantez, et al. Design and implementation of a smart meter with demand response capabilities.Energy Procedia 2016;103:195-200.

[13] Madeline Martinez-Pabon, Timothy Eveleigh, Bereket Tanju. Smart meter data analytics for optimal customer selection in demand response programs. Energy Procedia, 2017;107:49-59.

[14] Fu Yang, Li Zhenkun, Wei Chunfeng. Optimal economic dispatch for microgrid considering shiftable loads. Proceedings of the CSEE 2014;34(16):2612-2620.

[15] Zeng Bo, Hu Qiang, Liu Wenxia, et al. Dynamic probabilistic energy flow calculation for interconnected Electricity-Gas energy system considering complex uncertainties of demand response. Proceedings of the CSEE 2019:1-13.

[16] Xu Hang, Dong Shufeng, He Zhongxiao, et al. Electrothermal Comprehensive Demand Response Based on Multi-energy Complementarity. Power System Technology 2019;43(02):480-489.

[17] Yongli Wang, Yuding Wang, Huang Yujing, et al. Optimal scheduling of the regional integrated energy system based on energy price demand response. IEEE Transactions on Sustainable Energy 2018.

[18] Pan Zhang, Xun Dou, Wenhao Zhao, et al. Analysis of power sales strategies considering price-based demand response. Energy Procedia 2019;158:6701-6706.

[19] Kangping Lia, Liming Liu, Fei Wang, et al. Impact factors analysis on the probability characterized effects of time of use demand response tariffs using association rule mining method, Energy Convers Manag. 2019;197: 111891. https://doi.org/10.1016/j.enconman.2019.111891.

[20] Xing zhu, Lanlan Li, Kaile Zhou, et al. A meta-analysis on the price elasticity and income elzsticity of residential electricity demand. Journal of Cleaner Production 2018; 201:169-177.

[21] M. M. Eissa. Developing incentive demand response with commercial energy management system(CEMS)based on diffusion model, smart meters and new communication protocol. Applied Energy 2019;236:273-292.

[22] Cui Pengcheng, Shi Junyi, Wen Fushuan, et al. Optimal energy hub configuration considering integrated demand response. Electric Power Automation Equipment 2017;37(6):101-109.

[23] Song Yangyang, Wang Yansong, Yi Jingbo. Microgrid energy source optimization planning considering demand side response and thermo-electrical coupling. Pwer System Technology 2018;42(11):3469-3476.

[24] AmirAli Nazari, Reza Keypour. A two-stage stochastic model for energy storage planning in a microgrid incorporating bilateral contracts and demand response program. Journal of Energy Storage 2019;21:281-294.

[25] Andrew S, Ryan H. Analytical frameworks to incorporate demand response in long-term resource planning. Utilities Policy 2014; 28: 73-81.

[26] Joao A, Diana N, Carlo S, et al. Modeling the long-term impact of demand response in energy planning: The Portuguese electric system case study. Energy 2018; 165: 456-468.

[27] Ville O, Jussi E, Aira H, et al. Utilising demand response in the future finnish energy system with increased shares of baseload nuclear power and variable renewable energy. Energy 2018; 164:204-217.

[28] Diesel. Approximate natural gas generator fuel consumption chart[EB/OL]. [2019-02-14].https://www. dieselserviceands upply. com/Natural_Gas_Fuel_Consumption.aspx.

[29] M. Alipour, Z. Kazem and S. Heresh, A multi-follower bilevel stochastic programming approach forenergy

management of combined heat and power micro-grids Energy 2018; 149: 135-146.

[30] M. Alipour, Z. Kazem, Z. Hamidreza, et al. Hedging Strategies for Heat and Electricity Consumers in the Presence of Real-Time Demand Response Programs, IEEE Trans. Sustainable Energy 2019; 10(3): 1262-1270.

[31] Zhang C, Xu Y, Dong Z Y, et al. Robust coordination of distributed generation and price-based demand response in microgrids[J]. IEEE Transactions on Smart Grid, 2018, 9(5): 4236 – 4247.

[32] Farid V, Mehrdad S N, Alireza H, et al. Distributed energy resource and network expansion planning of a CCHP based active microgrid considering demand response programs. Energy 2019; 172: 79-105.

[33] Yongli W, Yudong W, Yujing H, et al. Plannning and operation method of the regional integrated energy system considering economy and environment. Energy 2019; 171: 731-750.